ELSEVIER

Catalysis Today 45 (1998) 319–325

CATALYSIS TODAY

Accelerated deactivation of hydrotreating catalysts: comparison to long-term deactivation in a commercial plant

Y. Tanaka[a,*], H. Shimada[b], N. Matsubayashi[b], A. Nishijima[1,b], M. Nomura[c]

[a]*Showa Shell Sekiyu K.K., 123-1, Shimokawairi, Atsugi-shi, Kanagawa 243-02, Japan*
[b]*National Institute of Materials and Chemical Research (NIMC), 1-1, Higashi, Tsukuba, Ibaraki 305, Japan*
[c]*Photon Factory, Institute of Materials Structure Science, 1-1, Oho, Tsukuba, Ibaraki 305, Japan*

Abstract

Accelerated deactivation tests of a laboratory prepared Co–Mo/Al_2O_3 catalyst were performed using three kinds of petroleum feedstocks. A high reaction temperature employed in the accelerated aging resulted in large amounts of carbonaceous deposition with high aromaticity, which were found to be the major deactivation cause. However, the effect of carbonaceous deposition during accelerated deactivation tests might have been overestimated compared with that during practical hydrotreating. When the catalysts were aged in a H_2S/H_2 stream without petroleum under the same reaction conditions, the crystal growth of MoS_2 layered structures was significant, but this rather resulted in an increase of both *k* (HDS) and *k* (HY). It was also suggested that the crystal growth during a commercial hydrotreating run was unlikely to be the major cause of catalyst deactivation.

Keywords: Accelerated deactivation; Hydrotreating; Co-Mo/Al_2O_3; Carbonaceous deposit; Structural change

1. Introduction

Elucidation of the catalyst deactivation causes during hydrotreating petroleum fractions is one of the most important issues to improve the catalytic performances in petroleum refining processes. In general, the deactivation causes have been considered to be the accumulation of carbonaceous and metallic deposition and the structural changes of the catalyst components [1]. However, questions still remain regarding to what extent each deactivation cause contributes to the total catalyst deactivation. Quantitative understanding of the catalyst deactivation cause is now essential for further development of long-life catalysts.

From this point of view, we carried out detailed analytical studies on the catalysts used in a commercial hydrodesulfurization (HDS) plant for one year [2,3]. In these studies, several kinds of laboratory prepared Co–Mo/Al_2O_3 and Ni–W/Al_2O_3 catalysts were fully analyzed by many characterization techniques and catalyst activity tests. As the result, we suggested that the structural change of the catalyst might be an important deactivation cause in addition to the carbonaceous and metallic deposition. The present study has been conducted to elucidate the contribution of the structural change of the catalyst. Through the comparison of the catalysts used in accelerated deactivation conditions and that used in

*Corresponding author.

[1]Present address: Kochi Prefectural Industrial Technology Center, Nunoshida, 3992-3, Kochi 781-51, Japan.

0920-5861/98/$ – see front matter
PII: S0920-5861(98)00239-9

the above commercial run, we discuss the effects of carbonaceous deposition and structural change of the catalysts on catalyst deactivation. In addition, we aim to point out differences in the catalyst deactivation behavior during the accelerated aging and practical hydrotreating.

2. Experimental

2.1. Accelerated aging test

The catalyst used was a laboratory prepared Co–Mo/Al_2O_3 with 5.3 wt% of Co as CoO and 20.7 wt% of Mo as MoO_3. The catalyst preparation method was already reported in the previous paper [2]. The feedstocks used in the present study were light gas oil (LGO, S: 1.20 wt%), vacuum gas oil (VGO, S: 2.64 wt%, CCR: 0.08 wt%) and vacuum gas oil containing atmospheric residue (VGO+AR, S: 2.68 wt%, CCR: 0.54 wt%, Ni: 0.5 ppm, V: 1.9 ppm).

Two modes of accelerated deactivation tests were carried out using micro-scale reactors with a catalyst capacity of 20 cm^3. The first mode of the tests was performed at 693 K for a total reaction time of 500 h with a H_2 pressure of 5.9 MPa, LHSV of 2.0 h^{-1} and H_2/oil ratio of 300 Nm^3/kl. The operation at 693 K was preceded by catalyst presulfiding at 523 K for 12 h by $(CH_3)_2S_2$ mixed gas–oil and gradual temperature raising for 81 h from 523 to 693 K by four steps. To discuss the effect of the catalyst structural changes apart from that of the carbonaceous materials, a catalyst aging run was performed in a stream of H_2S/H_2 without petroleum feedstocks. In the H_2S/H_2 treating, the catalyst was exposed to a flow of 3 Nl/h of 5% H_2S/H_2 mixture with the same total pressure and temperature profile as those for hydrotreating petroleum feedstocks. In the second mode, the catalyst aging was stopped at 633 K when the total reaction time reached 30 h. After the end of each reaction, the catalyst was taken out of the reactor and transferred to a vessel filled with diesel oil. The immersed catalyst was washed by toluene just prior to characterization. Thus, eight kinds of aged catalysts were prepared. Each catalyst was named, for instance, as VGO-30 or H_2S-500 herein after. The feedstock properties of the commercial run was similar to those of VGO+AR. The details of the commercial HDS run were already described in the previous paper [2].

2.2. Activity tests and characterization of aged catalysts

The HDS and hydrogenation (HY) activities of the catalysts were evaluated, respectively, by performing HDS of dibenzothiophene and HY of 1-methylnaphthalene in a batch-type autoclave. The experimental conditions were already reported [2]. Surface area (SA), total pore volume (PV), XPS spectra and CP/MAS-^{13}C-NMR spectra were obtained using a Bel Japan Belsorp28, a Shimadzu Autopore9220, a Phi 5600 spectrometer and a Bruker MSL-300 spectrometer, respectively. The details of Mo and Co K-edge EXAFS measurements and analyses were described in a previous paper [4]. TEM observations of the catalysts were performed on a JEOL JEM-3010 with a 300 kV electron beam at a total magnification of 1 800 000.

3. Results

3.1. Catalytic activity tests

Fig. 1(a) shows the HDS and HY rate constants of the catalysts used in accelerated deactivation tests. Among the catalysts with short aging (30 h), both activities decreased with increasing heavy components in the feedstocks. The activities of the catalysts used in petroleum hydrotreating further decreased after 500 h aging as shown in Fig. 1(b). The hydrotreating of LGO deactivated the catalyst more significantly than that of VGO after 500 h. In contrast to the petroleum hydrotreating, the activities of the catalyst treated in the H_2S/H_2 stream increased after 500 h of aging.

3.2. Catalyst characterization

3.2.1. Carbonaceous and metallic deposition

Table 1 summarizes the physical properties and carbonaceous and metallic deposition on the catalysts used in accelerated aging tests. Among the catalysts with short aging, the surface area and pore volume of the catalyst decreased with increasing the heavy

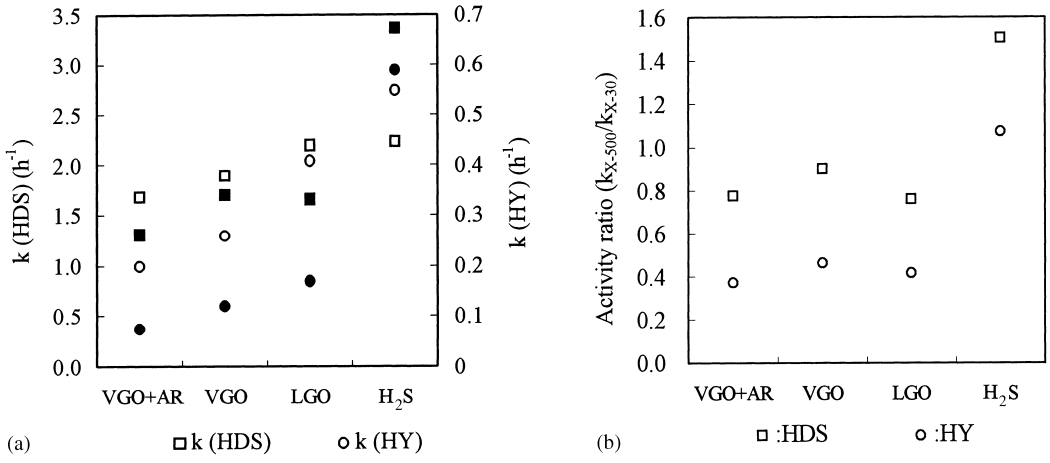

Fig. 1. (a) HDS and HY activities of aged catalysts (open: 30 h, solid: 500 h). (b) Relative deactivation of aged catalyst used for 500 h relative to aged catalyst used for 30 h.

Table 1
Physical properties and metallic and carbonaceous deposition on aged catalysts

	SA (m^2/g)	PV (ml/g)	NiO (wt%)	V_2O_5 (wt%)	C (wt%)	Aromatic (%)[b]	Aliphatic (%)
VGO+AR-30	152	0.440	0.01	0.04	8.9	21.8	78.2
VGO-30	160	0.467	0.01	<0.01	6.3	24.8	75.2
LGO-30	164	0.529	0.01	<0.01	3.8	20.6	79.4
H_2S-30	154	0.502	0.01	<0.01	1.0	—	—
VGO+AR-500	123	0.316	0.09	0.40	19.0	84.7	15.3
VGO-500	146	0.411	0.01	0.02	12.1	61.3	38.7
LGO-500	151	0.408	0.01	<0.01	11.2	68.4	31.6
H_2S-500	152	0.495	0.01	<0.01	1.2	—	—
COM[a]	152	0.349	0.40	2.30	7.9	49.0	51.0

[a]Catalyst used in the commercial run.
[b]Measured by CP/MAS-^{13}C-NMR.

components in the feedstocks. For the catalysts used in petroleum hydrotreating, both of the values further decreased after long aging. More significant pore-plugging was observed for LGO-500 than for VGO-500. The amount of the carbonaceous deposit increased with increasing the heavy components in the feedstocks for both series of the catalysts. The aromaticity of the carbonaceous deposit was very low for the catalysts used in short aging and significantly increased after long aging. The carbonaceous deposit on VGO+AR-500 exhibited extremely high aromaticity, perhaps because the deposited matters were subject to dehydrogenation at the high reaction temperature of 693 K. LGO-500 gave almost same amount of carbon deposition and higher aromaticity compared with VGO-500.

In summary, the heavy fractions in the feedstocks caused significant carbonaceous deposition with high aromaticity, which reduced the surface area and pore volume of the catalysts. Larger amounts of carbon observed for long aging are likely attributed to the high final temperature of long aging (693 K) compared with short aging (633 K). Serious coking observed for LGO-500 is also due to the high reaction temperature. Thus, extreme reaction conditions used for accelerated aging tests might have lead to

Table 2
MoS_2 structureal parameters obtained from TEM photographs

	L_{ave}[a] (nm)	N_{ave}[a]	Aspect ratio[a]	σ[b]	Σ[c]
VGO+AR-30	3.9	2.4	0.62	64	4.9×10^4
VGO-30	3.9	2.3	0.59	68	4.7×10^4
LGO-30	3.7	2.3	0.62	85	5.4×10^4
H_2S-30	3.8	2.9	0.76	99	8.5×10^4
VGO+AR-500	5.0	1.7	0.34	74	7.0×10^4
VGO-500	4.7	1.8	0.38	86	7.1×10^4
LGO-500	4.7	2.4	0.51	52	6.5×10^4
H_2S-500	4.1	3.1	0.76	105	1.2×10^4
COM.	5.2	2.9	0.55	94	1.5×10^5

[a]See text.
[b]σ, MoS_2 stack density (number of observed stacks per 10 000 nm^2).
[c]Σ, MoS_2 density which is calculated using L_{ave}, N_{ave} and σ.
These numbers were obtained from photographs with three different fields with 102 nm×76 nm.

overestimation of the effect of carbonaceous deposition on catalyst deactivation.

3.2.2. *Structural change of catalyst*

To quantitatively discuss the TEM results, the parameters shown in Table 2 have been obtained by measuring the number and length of MoS_2 fringes in each TEM photograph according to the method in the literature [5]. For each feedstock, long aging caused increases in L_{ave} (the average stack size in the lateral direction) and decreases in N_{ave} (the average number of layers per a stack), which resulted in eminent changes in the aspect ratio (N_{ave}/L_{ave}). An increase in L_{ave} directly corresponds to the growth of MoS_2 crystallites in the lateral directions. A decrease in N_{ave} indicates the formation of new single-layer MoS_2 crystallites from invisible small MoS_2 clusters.

The effects of the feedstocks on the parameters were not evidently observed except that the aspect ratio decreased with increasing heavy components in the feedstocks. The evident feature of the catalysts treated in the H_2S/H_2 stream was found in the large Σ values (MoS_2 density, the number of observed Mo atoms per 10 000 nm^2), which were attributed to relatively small numbers of invisible MoS_2 clusters. This indicates that the aggregation of small MoS_2 clusters during H_2S treating is much faster than that during petroleum hydrotreatment. In addition, H_2S-30 and H_2S-500 exhibited significantly higher aspect ratios than the catalysts used in hydrotreating petroleum. By H_2S treatment, MoS_2 crystallites grew preferentially in the normal directions to the layers. In contrast, petroleum hydrotreating promoted the MoS_2 crystal growth in the lateral directions.

COM gave a much larger Σ value than the catalysts used in accelerated aging tests. Although the final temperature of the commercial run (673 K) was lower than that of the present aging tests, much longer reaction period caused significant aggregation of invisible MoS_2 clusters to the layered structures. The aspect ratio of COM was smaller than that for short aging but larger than that for long aging. On this respect further discussion will be made elsewhere.

Fig. 2 shows the coordination numbers of sulfur (N(S)) and molybdenum (N(Mo)) around molybdenum obtained from the magnitudes of Fourier transformed Mo K-edge EXAFS spectra. The N(S) and N(Mo) values of the catalysts used in long aging were significantly higher than those for short aging. Both of the values were almost same for the petroleum treated catalysts, though H_2S-30 gave a slightly higher N(S) than the other catalysts used in short aging. The N(S) and N(Mo) of the catalyst used in a commercial run were almost same as those of the catalysts used in long aging.

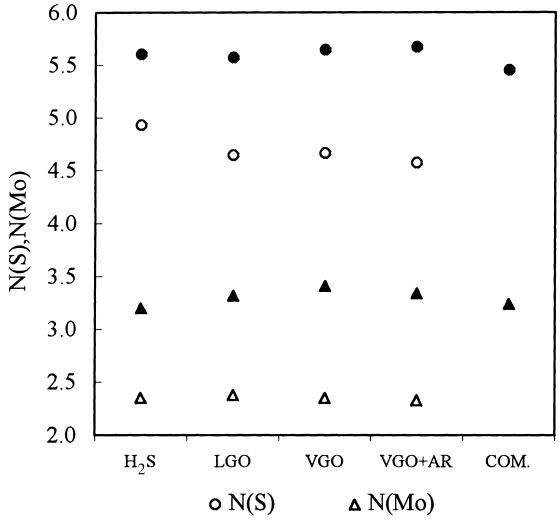

Fig. 2. N(S) (○) and N(Mo) (△) values of the catalysts obtained from Mo EXAFS (open: 30 h, solid: 500 h).

N(S) corresponds to the degree of Mo sulfidation in the catalyst. The increases in N(S) from short aging to long aging indicate progress of Mo sulfidation during this period. The increase in N(Mo) represents the crystal growth of the MoS_2 structure, though the crystal sizes estimated by N(Mo) values are not equal to the sizes in TEM photographs [6].

In the Co K-edge XANES spectra, all the catalysts gave quite similar features, which indicated mostly sulfide containing a small portion of oxide. Careful observation of Fourier transformed Co K-edge EXAFS spectra indicated slight increases in the distance between Co and the nearest neighbor atom from 30 h aging to 500 h aging. For the catalysts used in petroleum hydrotreating the distance was changed from 0.207 to 0.211 nm, for the catalysts treated by H_2S from 0.211 to 0.213 nm. This perhaps corresponds to the change of Co–O to Co–S bonding for a part of Co species. The formation of the CoS_2 or Co_9S_8 crystal structures leads to the nearest neighbor peak at 0.224 or 0.227 nm due to the scattering from the next nearest neighbor Co. Thus, the nearest neighbor peak at 0.207–0.213 nm precludes significant growth of cobalt sulfide crystalline structures.

Table 3 gives the sulfur contents together with XPS results. The increases in sulfur contents and the decrease in Mo^{6+} ratio from 30 to 500 h indicate progress of Mo sulfidation in this period. Also, the Co 2p XPS spectra (not shown here) exhibited the change of a part of cobalt oxide to cobalt sulfide in this period. These observations are quite consistent with the Mo K-edge and Co K-edge EXAFS results. Evident differences were observed in the S/Mo and Mo^{6+} ratios between VGO+AR treated catalysts and other catalysts. High S/Mo ratios observed for VGO+AR-30 and -500 are probably accounted for by the selective deposition of Ni and V on the external surface. The metallic contaminants were rapidly deposited on the external surface, and then diffused into the bulk. High ratios of Mo^{6+} observed for the VGO+AR treated catalysts were presumably related to the heavy components in the feedstocks. The AR matters were likely to change the local structure around molybdenum at the external surface, as already reported by the present authors [7].

Table 3
Sulfur contents and XPS analytical results of aged catalysts

	S (wt%)	S/Mo	Mo^{6+}/Total Mo
VGO+AR-30	9.2	3.4	0.26
VGO-30	9.4	2.1	0.22
LGO-30	9.0	2.2	0.22
H_2S-30	10.8	2.1	0.14
VGO+AR-500	9.9	3.3	0.18
VGO-500	9.7	2.3	0.12
LGO-500	9.8	2.5	0.11
H_2S-500	11.1	2.4	0.083
COM.	9.9	2.8	0.15

XPS analyses were made on the external surface of the catalyst extrudate.

The above characterization results give clear pictures of the MoS_2-like structures in the catalysts. Under all the conditions, the sulfidation of molybdenum species proceeded during 30 h aging and 500 h aging. The aging under the H_2S/H_2 stream sulfided the molybdenum species slightly faster than that under the petroleum hydrotreating. Growth of MoS_2 crystal structures proceeded in different manners under the two aging conditions. In hydrotreating petroleum feedstocks, relatively larger parts of molybdenum sulfide remained as small clusters and the growth of layered MoS_2-like structures was slow. The effect of feedstock properties on the crystal growth was not evident, but the aspect ratio decreased with increasing the heavy components in the feedstocks. In the aging under the H_2S/H_2 stream, the growth of layered MoS_2 crystal structure was fast and the structures had higher aspect ratios than those aged in hydrotreating petroleum.

4. Discussion

Fig. 3 shows the HYD activities of the aged catalysts as a function of the carbonaceous deposit. The tendency observed in Fig. 3 clearly demonstrates that the major deactivation cause during the accelerated aging is the carbonaceous deposition, though it is hard to separate the deactivation by pore plugging from that by direct active site poisoning. The decline of the profile is partly due to the change of the properties of the carbonaceous deposition from reactive hydrocarbon to refractory matters. The plot for COM in Fig. 3 is well consistent with the profiles obtained for the catalysts used in accelerated deactivation tests. Prob-

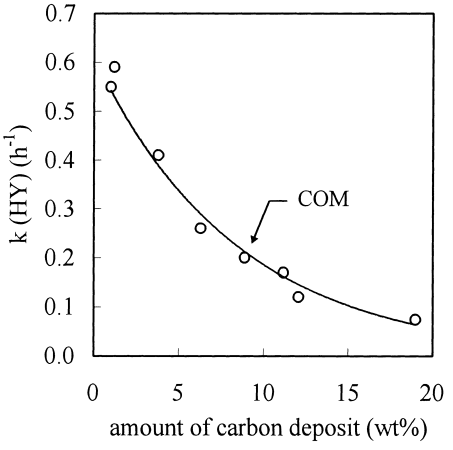

Fig. 3. Relationship between carbon deposit and k (HY).

ably, the deactivation of COM by metallic deposition is not significant, because the amount of the metallic deposition (2.5 wt%) is relatively small compared with the carbonaceous deposition (7.6 wt%).

The present results demonstrated that the activities of H_2S-500 with significant growth of MoS_2 crystalline structure were higher than those of H_2S-30 with less degree of crystalline growth. Some papers reported that an excess progress of sulfidation at high temperatures caused crystal growth which was unfavorable for the development of "Co–Mo–S" phases [8,9]. These studies claimed the decrease in the edge sites by high-temperature sulfiding based on the qualitative observation of the TEM photographs. As shown in Table 2, however, the H_2S treatment for a long period accelerated the crystal growth in the direction normal to the basal plane of the MoS_2 structure and rather increased the edge sites which were able to accommodate Co as the "Co–Mo–S" phases. These improvements of the activities by deep sulfiding may be related to the change in the structure from "Co–Mo–S-I" to "Co–Mo–S-II" as indicated in [10,11].

The decrease in the aspect ratio of MoS_2 structures during accelerated aging might be a cause of catalyst deactivation. However, the low aspect ratios of the catalysts used in 500 h aging were presumably caused by the high reaction temperature, since the aspect ratio of COM was larger than these values. The crystal growth of the MoS_2 structure during the practical hydrotreating was unlikely to result in serious catalyst deactivation.

The present authors reported that hydrotreating of coal-derived liquids caused serious collapse of the active "Ni–W–S" phase [12]. Later, this phenomena was strongly related to the asphaltene and polar matters in coal-derived liquids [4]. A similar change was observed on the external surface of VGO+AR-500 as the increase in the Mo^{6+} ratio. However, as evidenced by the Co K-edge XAFS results in the previous study [2], serious deterioration of the "Co–Mo–S" phase was not observed even after one-year of HDS run. Relatively small concentrations of asphaltene in the petroleum feedstocks did not lead to serious structural changes of the catalyst active phase.

5. Conclusion

In summary, the accelerated aging tests resulted in serious carbonaceous deposition which was the major cause of the catalyst deactivation. This was partly due to the higher temperature of the accelerated aging than practical hydrotreating, indicating that the accelerated aging tests did not fully represent practical deactivation. The crystal growth of the MoS_2 structures during the accelerated aging might be a deactivation cause, however, the crystal growth in the practical conditions was unlikely to cause serious deactivation.

Acknowledgements

The authors greatly appreciate the cooperation of Koa Oil Co., for charging their laboratory prepared catalysts into a commercial HDS plant. The authors also thank Mr. T. Kameoka of Catalysts and Chemicals Industries, for the activity measurements, Mr. T. Ishii and Mr. Y. Yokoyama of Tonen Corporation for the TEM analyses. The EXAFS measurements have been performed under the collaboration agreement between the Institute of Materials Structure Science and Petroleum Energy Center in Japan.

References

[1] H. Topsøe, B.S. Clausen, F.E. Massoth, Hydrotreating catalysis: science and technology, in: J.R. Anderson, M.

Boudart (Eds.), Catalysis – Science and Technology, vol. 11, Springer, Berlin, 1996, p. 24.
[2] Y. Yokoyama, N. Ishikawa, K. Nakanishi, K. Satoh, A. Nishijima, H. Shimada, N. Matsubayashi, M. Nomura, Catal. Today 29 (1996) 261.
[3] H. Makishima, Y. Tanaka, Y. Kato, S. Kure, H. Shimada, N. Matsubayashi, A. Nishijima, M. Nomura, Catal. Today 29 (1996) 267.
[4] N. Matsubayashi, H. Shimada, T. Sato, Y. Yoshimura, M. Imamura, A. Nishijima, Fuel Processing Technol. 41 (1995) 261.
[5] S. Eijsbouts, J.J.L. Heinerman, H.J.W. Elzerman, Appl. Catal. A 105 (1993) 53.
[6] S.M.A.M. Bouwens, R. Prins, V.J.H. de Beer, D.C. Koningsberger, J. Phys. Chem. 94 (1990) 3771.
[7] H. Shimada, N. Matsubayashi, T. Sato, Y. Yoshimura, M. Imamura, T. Kameoka, A. Nishijima, Catal. Lett. 20 (1993) 81.
[8] R. Candia, J. Villadsen, N.-Y. Topsøe, B.S. Clausen, H. Topsøe, Bull. Chim. Soc. Belg. 93 (1984) 763.
[9] R.S. Prada, F. Delannay, P. Grange, B. Delmon, Polyhedron 5 (1986) 195.
[10] H. Topsøe, B.S. Clausen, Catal. Rev. Sci. Eng. 26 (1984) 395.
[11] S. Eijsbouts, Appl. Catal. A158 (1997) 53.
[12] H. Shimada, N. Matsubayashi, T. Sato, Y. Yoshimura, M. Imamura, M. Kameoka, H. Yanase, A. Nishijima, Jap. J. Appl. Phys. 32(2)(Suppl.) (1993) 463.